Article

TRANSACTIONS OF THE INSTITUTE OF MEASUREMENT & CONTROL

Transactions of the Institute of Measurement and Control
1–10

DOI: 10.1177/0142331219878048
journals.sagepub.com/home/tim
SAGE

Disturbance observer-based model prediction control with real-time modified reference for a piezo-actuated nanopositioning stage

Min Ming, Zhao Feng, Jie Ling and Xiaohui Xiao

Abstract

Piezo-actuated micro-/nanopositioning systems have been widely employed in diverse high-precision positioning applications. However, the inherent hysteresis nonlinearity seriously deteriorates the tracking performance of piezo-actuated stages. This paper presents the design, analysis, and validation of a novel control scheme termed model prediction control (MPC) with real-time modified reference based on disturbance observer (DOB) to suppress the hysteresis nonlinearity and model uncertainty, in which the nonlinear effects are treated as an unknown disturbance to the system. In order to remove the most of the interference and diminish the effect of noise, a DOB is designed for the non-minimum phase (NMP) system. Then the difference between the actual displacement and the output of the nominal model termed the residual error is estimated and used to modify the reference in real time for a better performance. By the proposed method, the model of the inherent hysteresis is not required and the controller is established based on the identified nominal model. Its effectiveness is validated through experimental investigations on a commercial nanopositioner. Experimental results show that the proposed method can improve the tracking performance of the piezo-actuated stage, as compared with the traditional MPC and DOB-based MPC.

Keywords

Piezo-actuated stage, hysteresis compensation, disturbance observer, non-minimum phase, model prediction control

Introduction

Piezo-actuated nanopositioning stages have been widely applied in many precision instruments, such as nanomanipulators (Kenton and Leang, 2012), scanning probe microscopies (SPMs) (Voigtländer, 2015), and atomic force microscopes (AFMs) (Mahmood and Moheimani, 2009), which are usually designed as flexure-hinge-guided mechanisms driven by piezoelectric actuators (PEAs) with the merits of small size, high positioning resolution and quick frequency response (Gu et al., 2016). However, the voltage actuation is dominantly used in practical applications, resulting in the lightly damped dynamics and nonlinearity of the stage. Damping control (Ling et al., 2018; Ling et al., 2019a; Ling et al., 2019b) achieves great tracking performance by improving the closed-loop bandwidth in small amplitude signal, where the nonlinearity can be ignored. In large travel tracking situation, the nonlinearity is particularly hysteresis effect. The hysteresis effect increasing with the amplitude and frequency of reference signal can greatly degrade the positioning (Cao and Chen, 2012). It is necessary to design an effective controller to cope with the nonlinearity for precise positioning and tracking.

A wide variety of control techniques has been developed to suppress the piezoelectric hysteresis effect in recent literatures. These approaches mainly contain hysteresis model-based feedforward control, hysteresis model-free feedback control and feedforward-feedback control. Typically, the hysteresis is modeled, and the feedforward control is completed based on the inverse hysteresis model (Rosenbaum et al., 2010; Wang et al., 2014) or the direct hysteresis model (Rakotondrabe, 2011; Xu, 2013). Although these feedforward controllers are direct and effective, the identification of an accurate hysteresis model is time consuming and sometimes the inverse model is not available. Iterative learning control (ILC) is also a popular feedforward controller, such as the model-data integrated iterative learning controller for flexible tracking (Feng et al., 2017) and position domain cross-coupled iterative learning control (Ling et al., 2017), which are suitable for repetitive reference tracking. And repetitive control (Feng et al., 2018) shows great performance for periodic reference input. In the model-free feedback control, the hysteresis effect is usually treated as a disturbance to a nominal model. In this way, available control methods are able to suppress the disturbance

School of Power and Mechanical Engineering, Wuhan University, P.R. China

Corresponding author:
Xiaohui Xiao, School of Power and Mechanical Engineering, Wuhan University, No.8 South Donghu Road, Wuchang District, Wuhan, Hubei Province 430072, P.R. China.
Email: xhxiao@whu.edu.cn

for better performance of the piezo-actuated stages. A model reference adaptive PID (Xiao et al., 2012) is designed to track the desired reference path, which is tuned based on intuitive desired performance and robustness. This controller can get a stable performance in the whole working range, while the long adaptive time may limit its application field. A nonlinear PID controller with an inverted hysteresis compensator is proposed and implemented (Tang and Li, 2015), in which the hysteresis nonlinearity modeling is conducted by using the Preisach theory. Sliding mode control (SMC) has attracted considerable attention owning to the ease of implementation and robustness to disturbance (Motamedi et al., 2011). It is usually dealt with a second-order system (Peng and Chen, 2014; Xu and Abidi, 2008). When it comes to a high order system and only the position information of the piezo-actuated system is available, the state observer is needed (Ghafarirad et al., 2011). The digital sliding mode control (DSMC) using the discrete z-domain form transform function requires the input-output data only (Xu, 2014). However, the DSMC can only apply to a minimum phase system and is sensitive to the initial position error and noise. Among these algorithms, model prediction control (MPC) algorithm is popular and widely adopted in the industrial process control (Niu et al., 2016). For instance, it has been successfully applied to compensate hysteresis nonlinearity of PEAs (Wills et al., 2007).

If the disturbance and uncertainties can be completely or partially estimated, such estimations should greatly facilitate their compensation by means of control. In literatures, the active disturbance rejection approaches are developed for improving control performance. For example, sliding mode observer is used to reconstruct stochastic process and output disturbance (Yang et al., 2018) and a novel descriptor reduced-order observer is used to obtain the estimation of state and sensor fault directly without any supplementary design (Yang and Yin, 2018). In addition, the authors use a sliding mode observer to eliminate the effects of simultaneous disturbances, actuator and sensor faults has been developed (Yin et al., 2017). A disturbance observer (DOB)-based slide-mode control is designed for a second order system to improve performance (Cao and Chen, 2014). MPC has a well-established theoretical foundation and possesses the following advantages: capability of handing multi-input-multi-output process, ability to control non-minimum system and deal with physical constraints in the generation of control actions, simplicity of implementation based on the identified nominal model (Yang et al., 2010). In Rana et al. (2014, 2015), MPC has been successfully applied to achieve faster imaging in AFMs, in which the scanning area is small so that the hysteresis is negligible. A feedforward-feedback control that combines the inverse hysteresis model and MPC is presented (Cao et al., 2013). And to avoid the computation of complicated inverse hysteresis model, the authors model the piezo-actuated stage as a total (Liu et al., 2016), in which the total model is nonlinear. However, the nonlinear MPC is more complicated with heavy calculation. In Liu et al. (2016), the extra work of dynamic linearization of neural network-based model is introduced to linearize the model at each sampling interval. The MPC with DOB is proposed to control the current of raymond mill, which is a system with large time delays (Niu et al., 2016). A compound control consisting of a feedforward compensation part based on DOB and a feedback regulation part based on MPC (DOB–MPC) is developed to control the ball mill grinding circuit, which is a multivariable system with couplings, time delays and strong disturbances (Yang et al., 2010). It is confirmed that MPC with DOB performs better than the only MPC in the presence of strong disturbance and uncertainty. Because of the complexity of the control system, the performance of those controllers containing DOB and MPC are verified only through simulation results in multiple scenes including nominal case and model mismatch case.

In terms of that, it can be concluded that the tracking performance of piezo-actuated nanopositioning system is limited by hysteresis nonlinearity and traditional MPC can only be applied to track exactly in small travel range. MPC combined with DOB can significantly improve control performance by compensating disturbance. However, due to the imperfection of the DOB compensation, the tracking error concluding partial hysteresis and model uncertainties may exist. Considering the difference between the actual output with DOB compensation control and nominal model output, the traditional MPC with the predefined trajectory as the reference can't achieve satisfactory tracking accuracy. The residual error should be estimated and considered. To overcome the above drawbacks, this paper employs the difference between the actual output and nominal model output to modify the reference in real time. Then, this paper proposed a composite control consisting of MPC with real-time modified reference and DOB. The nonlinearity of the piezo-actuated stage is compensated by DOB, and then the MPC with real-time modified reference realizes the accurate tracking task. The contribution of this paper rests on the development of a novel control scheme, MPC with real-time modified reference based on a DOB, and the application of the developed control scheme to the piezo-actuated stage for tracking different types of reference signals.

The remainder of this paper is organized as follows. In "Piezo-actuated nanopositioning system", system configuration and a brief description of the system are stated. The design procedure of the composite controller is dictated in "Composite control scheme". Experiment setup and experimental results are presented in "Application to a piezo-actuated nanopositioning stage" and the "Conclusion" concludes the paper.

Piezo-actuated nanopositioning system

System configuration

Piezo-actuated micro-/nanopositioning stage uses multiple piezoelectric actuators to drive parallel compliant mechanism connected to the execution unit directly, and multi-DOF outputs can be achieved. Research on this system has been gradually mature, and some have been commercialized.

Figure 1 shows a block diagram of a piezo-actuated nanopositioning system. Therein, (1) the flexure-hinge-guided mechanism is usually employed to provide motion by the elastic deformations; (2) the piezoelectric actuators are applied to realize the actuation by generating force on the mechanism due to its excellent advantages of the large output force, non-electromagnetic interference, fast response speed, easy realization of nanometer resolution; (3) the driver

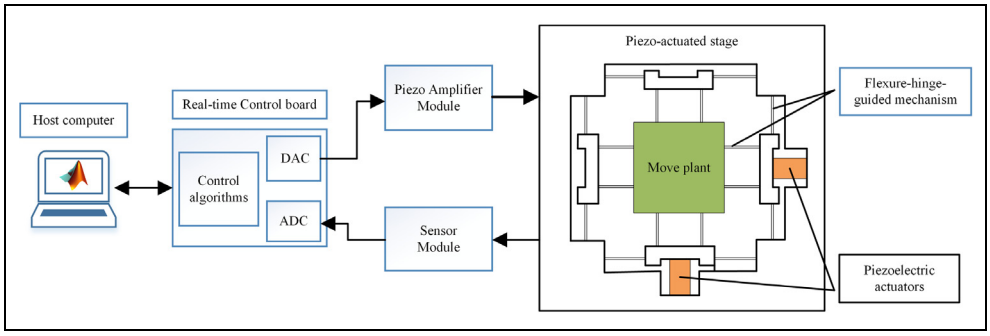

Figure 1. Block diagram of a piezo-actuated nanopositioning system.

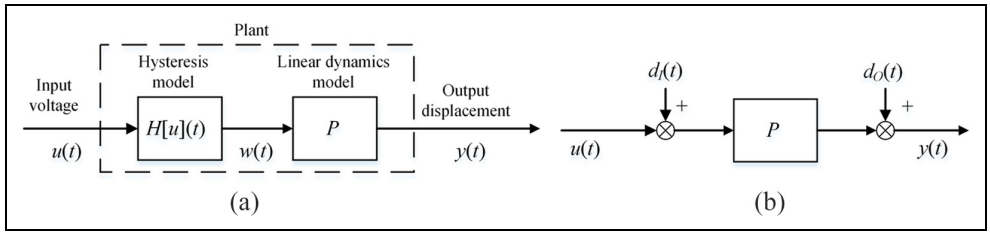

Figure 2. The model of piezo-actuated stage (a) Cascaded hysteresis model and linear dynamics model (b) The equivalent system model.

amplifier is used to amplify the control commands for the piezoelectric actuator; (4) the sensor is utilized to measure the real-time displacement of the mechanism; (5) the control algorithms are developed and implemented in the real-time control board to produce control commands for the piezoelectric actuator to achieve the nanopositioning motion of the flexure-hinge-guided mechanism.

System description

The usual model of the piezo-actuated stage is shown in Figure 2(a), where $H[u](t)$ denotes the hysteresis model, P represents the linear dynamics model. $u(t)$, $w(t)$, $y(t)$ are the input voltage, unmeasurable hysteresis output, and displacement output respectively. When treating the hysteresis effect and model uncertainty as disturbance, the system can be represented by the system in Figure 2(b). $d_I(t)$ and $d_O(t)$ denote the input and output disturbance. The controller can be designed and complemented for the linear dynamics model easily.

Composite control scheme

A composite control is proposed to control the piezo-actuated stage. It enhances the performance of the MPC-based feedback control by adding a DOB. The identified model of the stage is non-minimum phase (NMP). However, the inverse function of the NMP part is unstable. It resorts to DOB design with the consideration of NMP system (Zhou et al., 2012).

DOB for NMP system

The block diagram of the standard DOB is shown in Figure 3, where $P(z)$ is the real plant to be controlled and $P_n(z)$ is the nominal model, and $Q(z)$ is the low-pass filter. It can be seen that the procedure of the DOB closes a loop around the

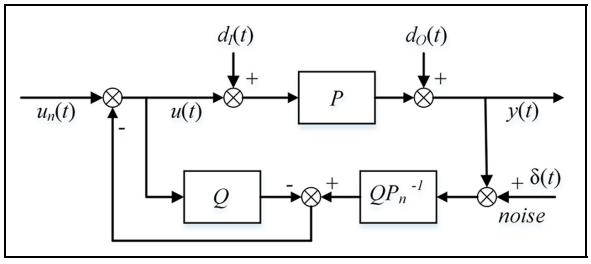

Figure 3. The block diagram of the standard DOB.

controlled plant to reject disturbances and force the input–output characteristics of this loop to approximate the nominal plant model. $P_n{}^{-1}(z)$ is the approximate inverse of the nominal model. The zero-phase-error tracking controller (ZPETC) technique is used to obtain the approximate inverse through converting NMP zeros of the model into stable zeros of the approximate inverse.

First, we write the dynamics of the system as in equation (1), partitioning $B(z)$ into the polynomial $B_s(z)$ containing the stable (invertible) zeros and the polynomial $B_u(z)$ containing the unstable (noninvertible) zeros

$$P_n(z) = \frac{B(z)}{A(z)} = \frac{B_s(z)B_u(z)}{A(z)} \tag{1}$$

The polynomial $B_u(z)$ contains m unstable zeros. Then, the polynomial $B_f(z)$ contains m stable zeros is obtained by reflecting the roots z_i of $B_u(z)$ into the unit circle to $1/z_i$. According to the ZPETC, the inverse model is

$$P_n{}^{-1}(z) = K\frac{A(z)B_f(z)}{B_s(z)} \tag{2}$$

$$K = 1 \Big/ \left(B_u(z)|_{z=1}\right)^2 \tag{3}$$

Where, K is scalar that compensates for losses in the DC gain. For convenience, the variable z is omitted in the following.

It can be seen that ${P_n}^{-1}$ is not causal. In this design, Q is specified as

$$Q = Q_0 z^{-d} \tag{4}$$

in which, Q_0 is a low-pass filter with the unit gain at low frequencies and the delay d is the relative order between numerator and denominator of ${P_n}^{-1}$.

This ensures that $Q_0{P_n}^{-1}$ is causal and the input signal and the estimated disturbance are coincident. The output of the plant can be expressed as follows

$$y = P(u + d_I) + d_O = Pu + d \tag{5}$$

$$u = u_n - \left[Q{P_n}^{-1}(y + \delta) - Qu\right] \tag{6}$$

In which, $d = Pd_{\mathrm{I}} + d_{\mathrm{o}}$ is the total disturbance. Then, the equation that relates the output y to the reference input u_n, disturbance d, and noise δ is

$$\begin{aligned} y &= \frac{P(1-Q)^{-1}u_n + d - P(1-Q)^{-1}Q{P_n}^{-1}\delta}{1 + P(1-Q)^{-1}Q{P_n}^{-1}} \\ &= T_{uy}u_n + T_{dy}d + T_{\delta y}\delta \end{aligned} \tag{7}$$

Where, T_{uy}, T_{dy}, and $T_{\delta y}$ are the transfer function from u_n to y, d to y and δ to y, respectively. The design of DOB is to obtain

$$y = P_n u_n \tag{8}$$

$$T_{dy} = \frac{1}{1 + P(1-Q)^{-1}Q{P_n}^{-1}} = 1 - \frac{PQ{P_n}^{-1}}{1 - Q + PQ{P_n}^{-1}} \tag{9}$$

$$T_{uy} = \frac{P(1-Q)^{-1}}{1 + P(1-Q)^{-1}Q{P_n}^{-1}} = \frac{1}{(1-Q)P^{-1} + Q{P_n}^{-1}} \tag{10}$$

$$T_{\delta y} = \frac{-P(1-Q)^{-1}Q{P_n}^{-1}}{1 + P(1-Q)^{-1}Q{P_n}^{-1}} \tag{11}$$

For the low-pass filter Q, it is assumed $Q = 1$ at low frequencies and $Q = 0$ at high frequencies. It can be obtained that $T_{uy} = P_n$ and $T_{dy} = 0$ for the low frequencies signal. And $T_{\delta y} = 0$ for high frequencies signal. This means the system has been regulated as the desired model eq. (8) for low frequency tracking signals. Namely, the DOB has compensated the disturbance effectively.

DOB-based MPC with real-time modified reference

The MPC acts as a feedback controller and is used to generate the manipulated control increment sequence at each sample time by minimizing the difference between the desired output and the predictive output. Only the first move is applied to the plant and this step is repeated for the next sampling instance. The proposed composite control is shown in Figure 4.

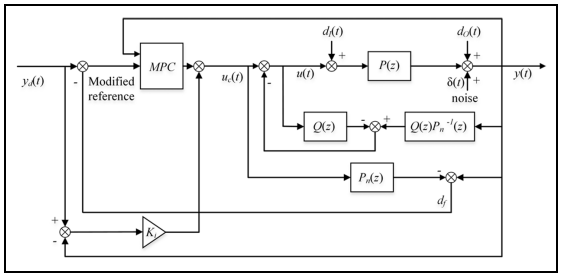

Figure 4. Block diagram of the proposed control scheme.

In this design, the nominal model of the plant is described by the state-space model

$$\begin{aligned} X(k+1) &= \mathbf{A}X(k) + \mathbf{B}U(k) \\ y(k) &= \mathbf{C}X(k) \end{aligned} \tag{12}$$

Making

$$\begin{cases} \Delta X(k+1) = X(k+1) - X(k) \\ \Delta y(k+1) = y(k+1) - y(k) \\ \Delta U(k+1) = U(k+1) - U(k) \end{cases} \tag{13}$$

Equation (12) can be rewritten as

$$\begin{cases} X_d(k+1) = \mathbf{A}_d X_d(k) + \mathbf{B}_d \Delta U(k) \\ y(k+1) = \mathbf{C}_d X_d(k) \end{cases} \tag{14}$$

Where, $X_d(k+1) = [\Delta X(k+1)\ y(k)]$, $\mathbf{A}_d$, $\mathbf{B}_d$, $\mathbf{C}_d$ are the augmented system matrices with

$$\mathbf{A}_d = \begin{bmatrix} \mathbf{A} & 0 \\ \mathbf{CA} & \mathbf{I} \end{bmatrix},\ \mathbf{B}_d = \begin{bmatrix} \mathbf{B} \\ \mathbf{CB} \end{bmatrix},\ \mathbf{C}_d = [0 \quad \mathbf{I}]$$

The predictive output sequence in the matrix form is then derived as

$$Y = \mathbf{F}X_d(k) + \mathbf{\Phi}\Delta U \tag{15}$$

in which

$$Y = \begin{bmatrix} y(k+1|k) \\ y(k+2|k) \\ \vdots \\ y(k+N_p|k) \end{bmatrix}\ \Delta U = \begin{bmatrix} \Delta u(k) \\ \Delta u(k+1) \\ \vdots \\ \Delta u(k+N_c-1) \end{bmatrix}\ \mathbf{F} = \begin{bmatrix} \mathbf{C_d A_d} \\ \mathbf{C_d A_d}^{\mathbf{2}} \\ \vdots \\ \mathbf{C_d A_d}^{\mathbf{N_p}} \end{bmatrix}$$

$$\Phi = \begin{bmatrix} \mathrm{C}_d\mathrm{B}_d & 0 & \cdots & 0 \\ \mathrm{C}_d\mathrm{A}_d\mathrm{B}_d & \mathrm{C}_d\mathrm{B}_d & \cdots & 0 \\ \vdots & \vdots & \ddots & \vdots \\ \mathrm{C}_d{\mathrm{A}_d}^{N_p-1}\mathrm{B}_d & \mathrm{C}_d{\mathrm{A}_d}^{N_p-2}\mathrm{B}_d & \cdots & \mathrm{C}_d{\mathrm{A}_d}^{N_p-N_c}\mathrm{B}_d \end{bmatrix}$$

N_p, N_c are the prediction horizon and the control horizon, respectively.

The DOB is designed based on the approximate inverse of the nominal model and the low-pass filter Q introduces the time delay d for the causality of the system. Partial

disturbance still exists after the system with DOB. Considering the residual disturbance, the reference trajectory is modified in real time in the proposed method. The prediction model in MPC is the identified nominal model. The disturbance rejection performance is achieved without sacrificing the nominal tracking performance.

The residual disturbance

$$d_f(k) = y(k) - P_n(k)u_c(k) \tag{16}$$

By assuming that the disturbance is slowly time varying and bounded, then the future disturbance values sequence in prediction horizon is estimated by

$$\zeta(k+1) = [\, d_f(k) \quad \cdots \quad d_f(k) \,] \tag{17}$$

The modified reference is derived as

$$R(k+1) = R_s(k+1) - \zeta(k+1) \tag{18}$$

in which, $R_s = [y_d(k+1|k) \quad y_d(k+2|k) \quad \cdots \quad y_d\big(k+N_p|k\big)]^T$,

$$R = \big[\, y_m(k+1|k) \quad y_m(k+2|k) \quad \cdots \quad y_m\big(k+N_p|k\big) \,\big]^T.$$

Using the aforementioned notations, the cost function for minimization can be expressed by,

$$J = [Y - R]^T W_Y [Y - R] + \Delta U^T W_U \Delta U \tag{19}$$

in which, W_Y and W_U are the adjustable weight matrices.

The control law is obtained by minimizing the value of the cost function J. If the constraints of the manipulated variable are not considered, the control law can be obtained by taking the derivative of the cost function and setting it to zero, that is

$$\frac{\partial J}{\partial \Delta U} = 0 \tag{20}$$

This results in

$$\Delta U = \big(\Phi^T W_Y \Phi + W_U\big)^{-1} \Phi^T W_Y (R(k) - Fx(k)) \tag{21}$$

By considering the constraints, the control increment ΔU can be solved by minimizing the cost function J, subject to the linear inequality constraints on the control input, that is

$$\begin{cases} u_{\min} \leqslant u(k+i-1) \leqslant u_{\max}, i = 1, \cdots, N_c \\ \Delta u_{\min} \leqslant \Delta u(k+i-1) \leqslant \Delta u_{\max}, i = 1, \cdots, N_c \end{cases} \tag{22}$$

$u_{\min}$ and $u_{\max}$ are the lower and upper bounds on the manipulated variable respectively, $\Delta u_{\min}$ and $\Delta u_{\max}$ lower and upper bounds on the control increments, respectively.

By considering the above equations, the constrained MPC problem can be expressed as a quadratic programming (QP) problem, similar to that in Rana et al. (2015).

The first entry of ΔU in Eq. (21) is used as the control increment for the next sampling interval

$$\Delta u(k) = \Psi R - \Psi F_2 y(k) - \Psi F_1 \Delta x(k) \tag{23}$$

Herein, the real control law can be written as follows

$$\begin{aligned} &u_c(k) = u_c(k-1) + \Delta u(k) \\ &\Rightarrow \big(1 - z^{-1}\big) u_c(k) = \Psi R - \Psi F_2 y(k) - \Psi F_1 \Delta x(k) \end{aligned} \tag{24}$$

In which, Ψ is the first row of $\big(\Phi^T W_Y \Phi + W_U\big)^{-1} \Phi^T W_Y$, $F = [\, F_1 \quad F_2 \,]$.

It can be seen that the control law is similar to a proportional control. When the PEA's model is not well described, the steady-state error is obvious. An integral type error compensation term is useful for reducing the steady-state error.

The error compensation term is defined as

$$\Delta u_e(k) = K_i(r_s(k) - y(k)) \tag{25}$$

In which, K_i is the gain of the integral term.

The final control law is obtained by adding the error compensation term

$$\big(1 - z^{-1}\big) u(k) = \Psi R - \Psi F_2 y(k) - \Psi F_1 \Delta x(k) + \Delta u_e(k) \tag{26}$$

$$u(k) = \Psi_1 R - \Psi_1 F_2 y(k) - \Psi_1 F_1 \Delta x(k) + \frac{K_i(r_s(k) - y(k))}{(1 - z^{-1})} \tag{27}$$

Where, $\Psi_1 = \Psi/(1 - z^{-1})$. It can be seen that the proposed predictive controller has an explicit form in each sampling interval.

Since MPC is designed according to the linear dynamic model of the piezo-actuated nanopositioning stage, the identified nominal model is required to match the real dynamic model well for perfect control performance. In addition, the control law is computed in each sampling interval. The sampling frequency and controller parameters, such as prediction horizon and the control horizon in MPC, should be set reasonably to avoid computational burden.

Application to a piezo-actuated nanopositioning stage

Experiment setup

The experimental setup is developed and shown in Figure 5. According to Figure 5, the setup is composed of a three-axis nanopositioner (P-561.3CD), a dSPACE MicrolabBox, a piezo amplifier module (E-503.00, Physik Instrumente) with a fixed gain of 10, a sensor monitor (E-509.C3A, Physik Instrumente) and the host PC. The control input voltage range is (0-10 V). And the output voltage range is (0-10 V), which is normalized with respect to 0-100μm. Details about the signal flow refer to Figure 5(b). The control algorithm is designed in Matlab/Simulink block diagram on the host PC, and then downloaded and executed on the target dSPACE MicroLabBox in the real-time software environment of dSPACE ControlDesk. When conducting experiments, only the x axis is adopted to implement the proposed controller and the sample rate is set to 10 kHz.

System identification

Since only the nominal model is required in the proposed control design, the AutoRegressive eXogenous (ARX) model is identified to describe the dynamics for x axis. To obtain the model parameters, a sine-sweep input voltage with a constant amplitude of 200 mV between 0.1 Hz and 500 Hz to the x axis. Notice that the low amplitude of the input voltage is used to excite the system for avoiding the effect of hysteresis nonlinearity. The input voltage and the output displacement

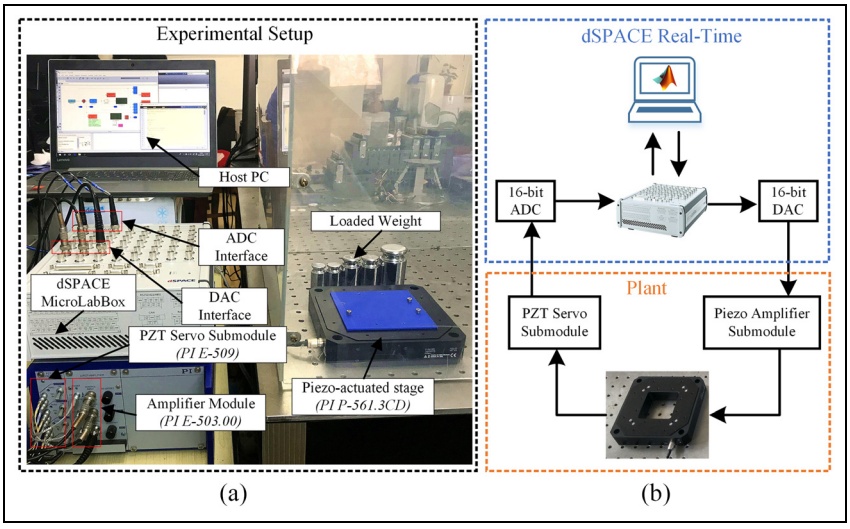

Figure 5. The experimental setup of the piezo-actuated stage (a) Experimental platform (b) Block diagram of the signal flow.

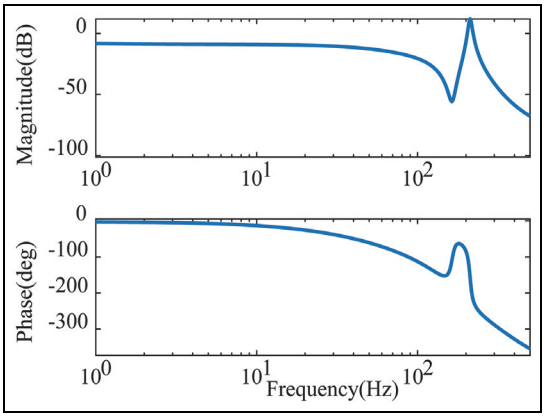

Figure 6. Bode plot of the identified linear dynamics model.

data taken from the sensor are imported to Matlab System Identification Toolbox to identify the model. The identified frequency response is shown in Figure 6. The discrete transfer function of the x axis is

$$P_x(z) = \frac{-0.007396z^5 + 0.04476z^4 - 0.06864z^3 + 0.02494z^2 + 0.02182z - 0.01546}{z^6 - 4.959z^5 + 10.68z^4 - 12.77z^3 + 8.905z^2 - 3.427z + 0.5666} \quad (28)$$

Subsequently, a controllable form of the system can be derived as equation (12), in which X is the sequence of system states, U is the sequence of input, and y is the output at the recent moment k. **A**, **B**, **C** represent the system matrices of the discrete state-space model.

Controller parameters

Based on the identified dynamic model, the proposed DOB-based MPC controller is to be tested in this section. Usually, the higher bandwidth of the low-pass filter can speed up the disturbance rejection. If the bandwidth is high, it will make the control system be too sensitive to measurement noise and even destroy the system stability. The bandwidth should be adjusted to a suitable parameter to achieve the desirable performance. In the experiments, the bandwidth is set as 80Hz. The prediction horizon N_p and the control horizon N_c are set as 4 and 3, respectively. These parameters can be determined by the trial-and-error method.

Results of tracking reference

In the verification experiments, three types of inputs are used as the reference signals for tracking. The first type of inputs is sinusoidal signals with different frequencies varying from 1 to 20 Hz. The second type of inputs is a piecewise signal consisting of different-amplitude sinusoidal signals with the same frequency (PS), as shown in Figure 7(a). The amplitudes of the second, third, fourth period and fifth period of the sinusoidal signals were 80%, 60%, 40% and 20% of the amplitude of the first period, respectively. The last type, shown in Figure 7(b), is a complex signal of three sinusoidal signals with different frequencies, amplitudes and phase delays (CS).

$$CS = 0.77\left(1 - \cos\left(\frac{2\pi f_{\max}}{9}t\right)\right) + 0.69\left(1 - \cos\left(\frac{10\pi f_{\max}}{9}t\right)\right) + 1.05(1 - \cos(2\pi f_{\max}t)) \quad (23)$$

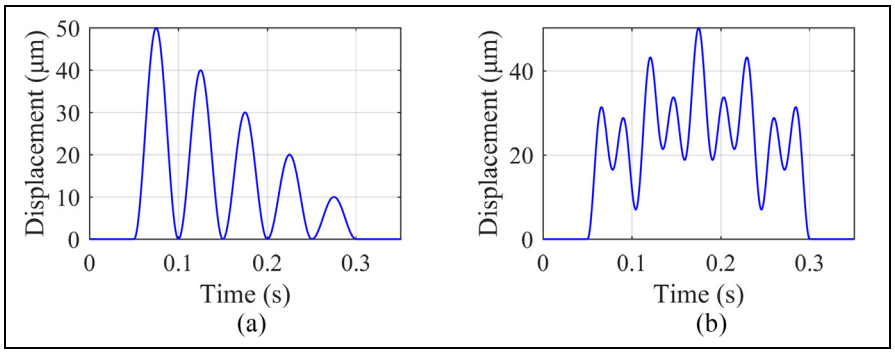

Figure 7. Reference inputs for the experimental verification (a) The piecewise signal (b) The complex signal.

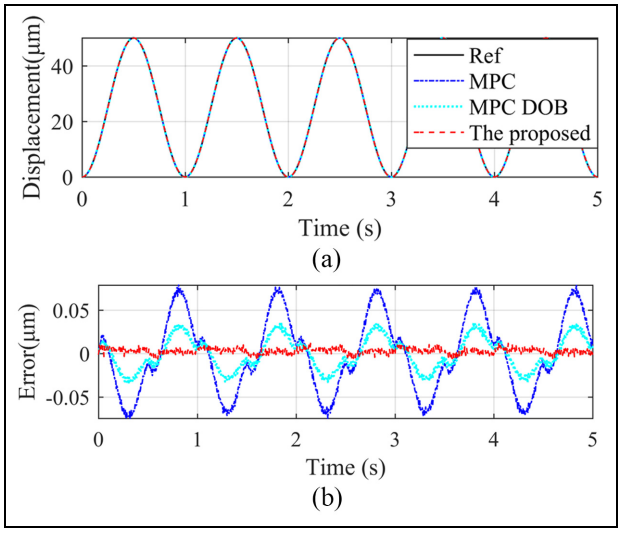

Figure 8. Experimental results with 1 Hz sine references (a) Reference and actual position trajectories (b) Tracking errors.

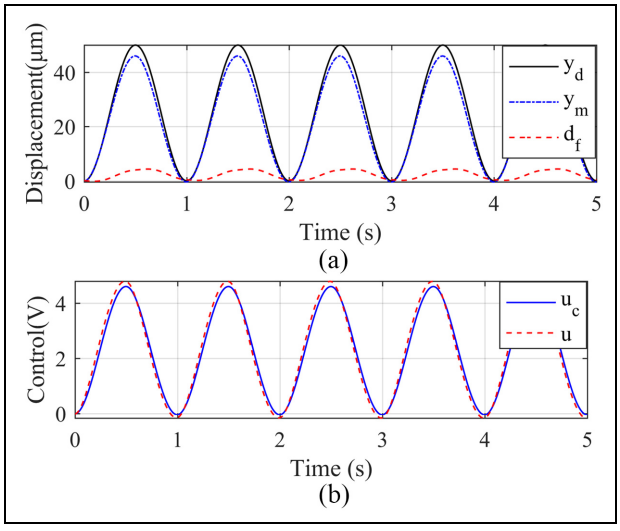

Figure 9. The proposed control with 1 Hz sine references (a) the modified references and the estimated residual disturbance (b) the control signals u_c and u.

And the proposed method is compared with the MPC (Rana et al., 2015) and the traditional MPC based on DOB (Niu et al., 2016). For a quantitative analysis, the tracking errors are calculated in terms of the root-mean-square (RMS) and the maximum (MAX) of the difference between the desired and measured outputs.

First, the motion tracking of sinusoidal signals with 1 Hz, 10Hz, and 20Hz is tested respectively.

Figure 8 shows the tracking performance for a 1 Hz, 50 μm sinusoidal input in the x axis. In Figure 8, it can be seen that all three control methods can effectively improve tracking performance. It is observed that the MPC method produces RMS and MAX error of 0.043 and 0.079 μm, that is, 0.086% and 0.158% of the motion range. The DOB-based MPC leads to RMS and MAX error of 0.019 and 0.037 μm, that is, 0.037% and 0.075% of the motion range. The proposed method achieves best performance with the RMS and MAX error of 0.005 and 0.015μm, equivalent to 0.009% and 0.030% of the motion range. As compared with the MPC method, the DOB-based MPC reduces RMS and MAX error by 55.8% and 53.2%, and the proposed method reduces RMS and MAX error by 88.4% and 81.0%.

Figure 9(a) shows the desired reference, the modified reference and the estimated residual disturbance with the proposed controller for tracking of 1 Hz sine. The control signal u_c (completed by MPC) and the control signal (MPC-based DOB) are included in Figure 9(b). It can be seen that the reference is modified in the real time, which promises the better performance. The difference between the modified reference y_m and the given reference y_d mainly because the gain changes and the uncompensated hysteresis display like the phase lag. The estimated residual disturbance is used to obtain the modified reference y_m, which is the reference for the MPC.

To further show the performance of the proposed method, the experiments are designed and implemented for the piecewise signal input and the complex signal. The results of tracking different-amplitude sinusoidal signals with the frequency of 10 Hz are shown in Figure 10 and these important signals are included in Figure 11.

The results of tracking a complex signal with the maximum frequency of 9 Hz are shown in Figure 12 and Figure 13. Similarly, the performance of the propose method is best,

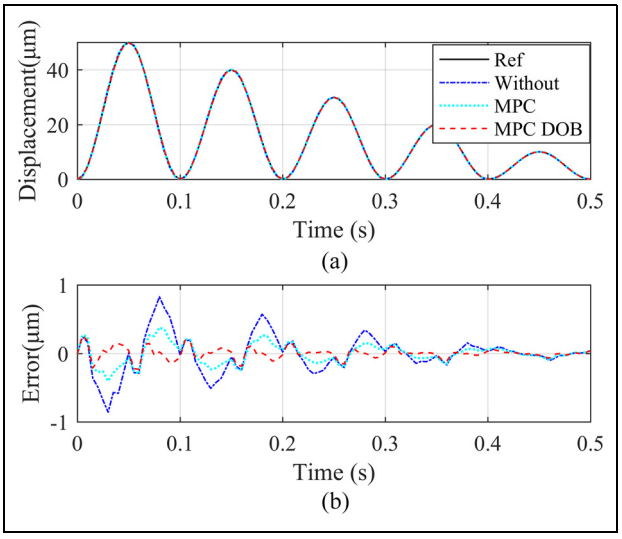

Figure 10. Experimental results with the 10 Hz piecewise signal (a) Reference and actual position trajectories (b) Tracking errors.

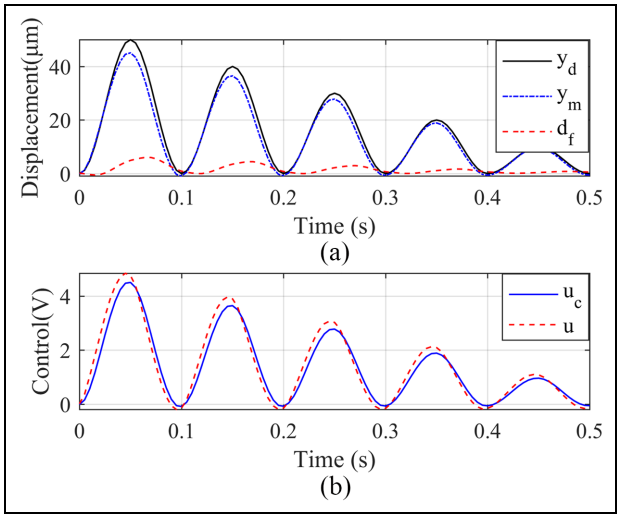

Figure 11. The proposed control with 10 Hz piecewise signal reference (a) the references and the estimated residual disturbance (b) the control signals u_c and u.

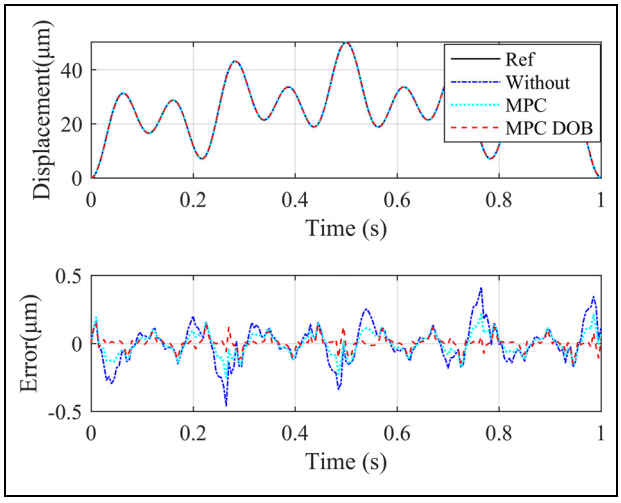

Figure 12. Experimental results with the complex signal with f_{max} = 9 Hz (a) Reference and actual position trajectories (b) Tracking errors.

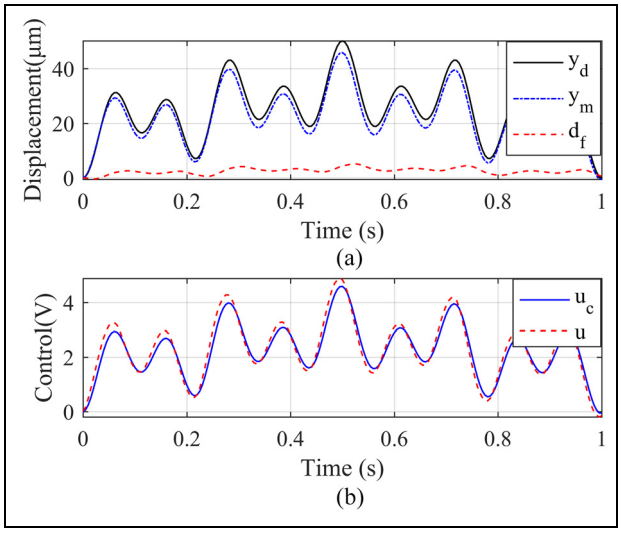

Figure 13. The proposed control with the complex signal with f_{max} = 9 Hz (a) the modified references and the estimated residual disturbance (b) the control signals u_c and u.

and the DOB-based MPC is better than the MPC in both cases.

The specific numerical results are presented in Table 1 and Table 2. For a clear presentation, Table 1 and Table 2 list the value of RMS and MAX tracking errors and the corresponding percentage versus to the motion range without control and with the three controllers. The RMS errors and percentage versus to the total stroke in Table 1, and the MAX errors and percentage versus to the total stroke in Table 2.

From Tables 1 and Table 2, it can be seen that the developed method performs better than MPC and MPC based on DOB. Performance improvements are evident when tracking signals of low frequency. However, it is not obvious for tracking signals of high frequency, for example, the sinusoidal signals with 20 Hz. As the amplitude and frequency of the tracking signal increase, the disturbance cannot be assumed slowly time varying. According to the perturbation estimation technique, the disturbance is estimated by its one-step delayed value and constant in prediction horizon, which is not enough accurate in applications for tracking signals of high frequency.

Experimental results of robustness test

In this subsection, these reference signals are fed into the closed-loop system under the proposed controller to test its robustness. The tracking error results included in Table 3 prove that this controller performs well against load

Table 1. The value of RMS tracking errors and percentage versus to the total stroke.

Signal(Hz)		MPC(μm / %)	MPC + DOB(μm / %)	The proposed MPC(μm / %)
Sine	1	0.043 / 0.086	0.019 / 0.037	0.005 / 0.009
	10	0.455 / 0.909	0.239 / 0.476	0.135 / 0.271
	20	1.166 / 2.292	0.880 / 1.759	0.645 / 1.298
PS	1	0.026 / 0.052	0.012 / 0.023	0.005 / 0.011
	10	0.278 / 0.556	0.152 / 0.303	0.087 / 0.175
	20	0.721 / 1.420	0.555 / 1.107	0.507 / 1.019
CS	f_{max} = 0.9	0.013 / 0.025	0.006 / 0.012	0.004 / 0.009
	f_{max} = 9	0.132 / 0.261	0.081 / 0.160	0.047 / 0.094

Table 2. The value of MAX tracking errors and percentage versus to the total stroke.

Signal(Hz)		MPC(μm / %)	MPC + DOB(μm / %)	The proposed MPC(μm / %)
Sine	1	0.079 / 0.158	0.037 / 0.075	0.015 / 0.030
	10	0.826 / 1.651	0.401 / 0.800	0.370 / 0.741
	20	2.689 / 5.285	1.882 / 3.760	1.473 / 2.950
PS	1	0.079 / 0.157	0.035 / 0.071	0.020 / 0.039
	10	0.826 / 1.652	0.407 / 0.812	0.368 / 0.736
	20	2.438 / 4.799	1.830 / 3.652	1.475 / 2.965
CS	f_{max} = 0.9	0.041 / 0.081	0.021 / 0.040	0.014 / 0.028
	f_{max} = 9	0.452 / 0.895	0.253 / 0.502	0.199 / 0.395

Table 3. The value of RMS tracking errors with the proposed control under different loads.

Signal(Hz)		0 g(μm)	100 g(μm)	150 g(μm)
Sine	1	0.005	0.005	0.005
	10	0.135	0.136	0.130
	20	0.645	0.761	0.797
PS	1	0.005	0.004	0.004
	10	0.087	0.087	0.086
	20	0.507	0.509	0.497
CS	f_{max} = 0.9	0.004	0.005	0.005
	f_{max} = 9	0.047	0.058	0.057

variations (100 g and 150 g) in the experiments. Herein, for a system with already known load variations, such as applications in microassembling, cell manipulation, SPM scanning where consistent positioning performance under different loads are demanded, the proposed controller can be considered as an alternative option for its robustness.

Conclusion

This paper presents the development of a composite control for control the piezo-actuated stage. It enhances the performance of the MPC-based feedback control by adding a DOB and modifying the reference based on the residual disturbance. First, an DOB is designed with the considerations of NMP of the nominal model. Then, the residual disturbance is estimated and used to modified the reference to the MPC. By the technique of MPC, the control law is solved in an explicit form in each sampling interval. The implement of the proposed control is convenient in practical applications. Further, the proposed method can be easily extended to the case of multiple-input-multiple-output (MIMO) systems. The tracking experiments are conducted on the constructed test platform. Comparison experiments illustrate the effectiveness of the proposed method. The future work will concentrate upon the improvement of disturbance estimation.

Declaration of conflicting interests

The author(s) declared no potential conflict of interests with respect to the research, authorship and/or publication of this article.

Funding

The author(s) disclosed receipt of the following financial support for the research, authorship, and/or publication of this article: This work was supported by Shenzhen Science and Technology Program (grant JCYJ20170306171514468).

ORCID iD

Xiaohui Xiao https://orcid.org/0000-0003-2398-8819

References

Cao Y and Chen XB (2012) A novel discrete ARMA-based model for piezoelectric actuator hysteresis. *IEEE/ASME Transactions on Mechatronics* 17(4): 737–744.

Cao Y and Chen X (2014) Disturbance-observer-based sliding-mode control for a 3-DOF nanopositioning stage. *IEEE/ASME Transactions on Mechatronics* 19(3): 924–931.

Cao Y, Cheng L, Chen XB, et al. (2013) An inversion-based model predictive control with an integral-of-error state variable for piezoelectric actuators. *IEEE/ASME Transactions on Mechatronics* 18(3): 895–904.

Feng Z, Ling J, Ming M, et al. (2017) High-bandwidth and flexible tracking control for precision motion with application to a piezo nanopositioner. *Review of Scientific Instruments* 88(8): 085107: 1–10.

Feng Z, Ling J, Ming M, et al. (2018) A model-data integrated iterative learning controller for flexible tracking with application to a piezo nanopositioner. *Transactions of the Institute of Measurement and Control* 40(10): 3201–3210.

Ghafarirad H, Rezaei SM, Abdullah A, et al. (2011) Observer-based sliding mode control with adaptive perturbation estimation for micropositioning actuators. *Precision Engineering* 35(2): 271–281.

Gu GY, Zhu LM, Su CY, et al. (2016) Modeling and Control of piezo-actuated nanopositioning stages: A survey. *IEEE Transactions on Automation Science & Engineering* 13(1): 313–332.

Kenton BJ and Leang KK (2012) Design and control of a three-axis serial-kinematic high-bandwidth nanopositioner. *IEEE/ASME Transactions on Mechatronics* 17(2): 356–369.

Ling J, Feng Z, Yao D, et al. (2018a) Non-linear contour tracking using feedback PID and feedforward position domain cross-coupled iterative learning control. *Transactions of the Institute of Measurement and Control* 40(6): 1970–1982.

Ling J, Feng Z, Ming M, et al. (2018b) Damping controller design for nanopositioners: A hybrid reference model matching and virtual reference feedback tuning approach. *International Journal of Precision Engineering and Manufacturing* 19(1): 13–22.

Ling J, Feng Z, Ming M, et al. (2019a) Model reference adaptive damping control for a nanopositioning stage with load uncertainties. *Review of Scientific Instruments* 90(4): 045101: 1–10.

Ling J, Rakotondrabe M, Feng Z, et al. (2019b) A Robust Resonant Controller for High-Speed Scanning of Nanopositioners: Design and Implementation. *IEEE Transactions on Control Systems Technology*.

Liu W, Cheng L, Hou ZG, et al. (2016) An inversion-free predictive controller for piezoelectric actuators based on a dynamic linearized neural network model. *IEEE/ASME Transactions on Mechatronics* 21(1): 214–226.

Mahmood I and Moheimani SR (2009) Making a commercial atomic force microscope more accurate and faster using positive position feedback control. *Review of Scientific Instruments* 80(6): 063705: 1–8.

Motamedi M, Ahmadian MT, Vossoughi G, et al. (2011) Adaptive sliding mode control of a piezo-actuated bilateral teleoperated micromanipulation system. *Precision Engineering* 35(2): 309–317.

Niu D, Chen X, Yang J, et al. (2016) Composite control for raymond mill based on model predictive control and disturbance observer. *Advances in Mechanical Engineering* 8(3): 1687814016639825: 1–10.

Peng JY and Chen XB (2014) Integrated PID-Based Sliding Mode State Estimation and Control for Piezoelectric Actuators. *IEEE/ASME Transactions on Mechatronics* 19(1): 88–99.

Rakotondrabe M (2011) Bouc–Wen modeling and inverse multiplicative structure to compensate hysteresis nonlinearity in piezoelectric actuators. *IEEE Transactions on Automation Science & Engineering* 8(2): 428–431.

Rana MS, Pota HR and Petersen IR (2014) Spiral scanning with improved control for faster imaging of AFM. *IEEE Transactions on Nanotechnology* 13(3): 541–550.

Rana MS, Pota HR and Petersen IR (2015) Performance of sinusoidal scanning with MPC in AFM imaging. *IEEE/ASME Transactions on Mechatronics* 20(1): 73–83.

Rosenbaum S, Ruderman M, Strohla T, et al. (2010) Use of Jiles–Atherton and Preisach hysteresis models for inverse feed-forward control. *IEEE Transactions on Magnetics* 46(12): 3984–3989.

Tang H and Li Y (2015) Feedforward nonlinear PID control of a novel micromanipulator using Preisach hysteresis compensator. *Robotics & Computer Integrated Manufacturing* 34: 124–132.

Voigtländer B (2015) *Scanning Probe Microscopy*. Springer, Berlin.

Wang G, Guan C, Zhang X, et al. (2014) Precision control of piezo-actuated optical deflector with nonlinearity correction based on hysteresis model. *Optics & Laser Technology* 57: 26–31.

Wills AG, Bates D, Fleming AJ, et al. (2007) Model predictive control applied to constraint handling in active noise and vibration control. *IEEE Transactions on Control Systems Technology* 16(1): 3–12.

Xiao S, Li Y and Liu J (2012) A model reference adaptive PID control for electromagnetic actuated micro-positioning stage. In: *2012 IEEE International Conference on Automation Science and Engineering (CASE)*. IEEE: 97–102.

Xu JX and Abidi K (2008) Discrete-time output integral sliding-mode control for a piezomotor-driven linear motion stage. In: *IEEE Transactions on Industrial Electronics* 55(11): 3917–3926.

Xu Q (2013) Identification and compensation of piezoelectric hysteresis without modeling hysteresis inverse. *IEEE Transactions on Industrial Electronics* 60(9): 3927–3937.

Xu Q (2014) Digital sliding-mode control of piezoelectric micropositioning system based on input–output model. *IEEE Transactions on Industrial Electronics* 61(10): 5517–5526.

Yang H and Yin S (2018) Descriptor Observers Design for Markov Jump Systems with Simultaneous Sensor and Actuator Faults. *IEEE Transactions on Automatic Control* 64(8): 3370–3377.

Yang H, Jiang Y and Yin S (2018) Fault-tolerant control of time-delay Markov jump systems with Itô stochastic process and output disturbance based on sliding mode observer. *IEEE Transactions on Industrial Informatics* 14(12): 5299–5307.

Yang J, Li S, Chen X, et al. (2010) Disturbance rejection of ball mill grinding circuits using DOB and MPC. *Powder Technology* 198(2): 219–228.

Yin S, Yang H and Kaynak O (2017) Sliding mode observer-based FTC for Markovian jump systems with actuator and sensor faults. *IEEE Transactions on Automatic Control* 62(7): 3551–3558.

Zhou P, Chai TY and Zhao JH. (2012) DOB Design for nonminimum-phase delay systems and its application in multivariable MPC control. *IEEE Transactions on Circuits & Systems II Express Briefs* 59(8): 525–529.